J. Astrophys. Astr. (2023) 44:70
https://doi.org/10.1007/s12036-023-09960-w

Protoplanetary disk formation in rotating, magnetized and turbulent molecular cloud

GEMECHU M. KUMSSA* and S. B. TESSEMA

Astronomy and Astrophysics Department, Space Science and Geospatial Institute (SSGI), Entoto Observatory and Research Center (EORC), P. O. Box. 33679, Addis Ababa, Ethiopia.
*Corresponding author. E-mail: gemechumk@gmail.com

MS received 22 February 2023; accepted 18 April 2023

Abstract. The study of protoplanetary disk formation and its connection with Solar system's origin is considered to be one of the longest-standing problems in astronomy and astrophysics. To the current human understanding, planets are believed to be the hosts of life. Therefore, understanding the dynamic process affecting the formation of protoplanetary disk leads to predicting the origin of our Solar system. The fundamental question we raise here is how the properties of the surrounding gas and dust, which provide mass for the disk and central protostar formations, affect the properties of the protoplanetary disk. This paper investigates how the infalling core's magnetic field, rotation and turbulence govern the protoplanetary disk formation. The theoretical model we have developed and the numerical results generated from the theoretical model show that a strongly magnetized and rotating core results in a relatively massive protoplanetary disk. Moreover, most of the disk's angular momentum is removed outwards due to the infalling core's magnetic field and its rotation speed.

Keywords. Protoplanetary disk—molecular cloud—magnetized core—momentum transport—turbulence.

1. Introduction

Throughout the lifetime of the the rotating circumstellar disk of dense gas surrounding a young newly formed star, which lasts a few million years, much of its mass drains onto the central protostar, while some condenses into planets and some is lost to outflows (e.g., protostellar jets, photo-evaporative winds and magnetic winds; Nixon *et al.* 2018).

The molecular clouds (MCs) fragment to form dense cores and they collapse under gravity to form protostars. Formation of circumstellar disk surrounding a protorar is attributed to the conservation of angular momentum (Anathpindika & Francesco 2013).[1]

Using three-dimensional numerical simulations, Bate (1998) and Inutsuka *et al.* (2010) have examined the disk creation by gravitational collapse. According to Joos *et al.* (2012), the magnetic field and core rotation can have an impact on how Keplerian disks form without turbulence. On the other hand, Seifried *et al.* (2013) noticed turbulence-induced disk formation in strongly magnetized cloud cores. However, our goal is to develop a theoretical model for the formation of protoplanetary disks in turbulent, magnetic and rotating molecular clouds.

Cassen (2006) has done theoretical work on the genesis and evolution of protoplanetary disks. The numerical simulations show that one-dimensional viscous accretion disk evolves, taking into account the impact of the cloud core's infall on the disk. However, each of the potential core pressure factors was taken into account separately. According to Nakamoto & Nakagawa (1994) and Zhu *et al.* (2010), the disk develops gravitational instability throughout its creation phase. The main aim of this work is to investigate the key factors causing this instability. Previous studies have employed the self-similar solution of the solitary isothermal sphere's mass accretion rate from the cloud core onto the disk (Shu 1977).

The cloud cores collapse and form a protostar surrounded by a disk of gas (protostellar disk) near their centers. These protostars are relatively big (au-size)

[1] Zhang *et al.* (2014) defined molecular clump as an entity of 1 pc that forms massive stars with a population of lower mass stars, and dense cores as an entity of 0.01–0.1 pc that forms one or a group of stars.

Published online: 03 July 2023

(Ward & Whitworth 2011). The typical masses of pre-stellar cores in low-mass star-forming regions like Taurus and Ophiuchus range from ∼0.5 $M_\odot$ to ∼10 $M_\odot$ (Ward & Whitworth 2011). In this work, we mainly focus on fragments of MCs, which are the sites of single stars and protoplanetary disks surrounding them. Planets form from gas and dust in protoplanetary disks (Armitage 2010).

Externally illuminated photo-evaporating protoplanetary disk of mass $M_d \sim 1\ M_\odot$ has been observed by Enoch *et al.* (2009). Moreover, Mann *et al.* (2015) surveyed NGC 2024 (age ∼0.5 Myr) and found a larger fraction of disks with masses of 0.01 $M_\odot$ and Walch *et al.* (2010) found protoplanetary disks of mass 0.03–0.05 $M_\odot$. On the other hand, Matsumoto & Hanawa (2003) obtained the central protostar of mass ∼0.01−0.1 $M_\odot$.

Apart from the mass, different properties of the protoplanetary disks were studied by different scholars, for instance, for Lupus, the relation between disk mass and accretion rate was studied by Williams & Best (2014) and Ansdell *et al.* (2016). The radial gas temperature profile $T(r)$ of the disk based on the data of the surface brightness profiles is provided by Gonzalez & Laibe (2015) and Nomura *et al.* (2016).

As presented by Kimura & Tsuribe (2012), two criteria are frequently used for discussing whether a protoplanetary disk is likely to fragment or not. The first is Toomre's stability criterion (Toomre 1964):

$$Q = \frac{a_T \kappa_{ep}}{\pi G \Sigma} > 1,$$

with the gravitational constant, G, epicyclic frequency, κ_{ep}, sound speed, $c_s = a_T$, surface density, Σ and stability parameter, Q. Toomre (1964) showed that the infinitesimally thin disk is stable if stability criterion $Q > 1$. On the other hand, Gammie (2001) suggested that rapid cooling is necessary for fragmentation, in addition to violating the Toomre criterion $Q > 1$.

We are unable to comprehend the processes involved in planet formation without a grasp of the physical laws and parameters governing the creation of the protoplanetary disk. This inspired us to research how the characteristics of the core affect protoplanetary disk formation. In this study, we address the challenge of describing the disk mass in terms of mass of the central core, thermal pressure, magnetic pressure, turbulence pressure and rotational pressure. In this study, the mass and angular momentum of the protoplanetary disk, which are produced from a revolving, magnetic and turbulent core, are calculated.

The common method we applied is theoretical modeling, followed by numerical calculation. Thus, we formulated the mass of the protoplanetary disk in terms of the protostar properties. First, we described the core accretion rate in terms of the magnetic field, turbulent speed, thermal temperature and speed of rotation of the core. Then, equated the core accretion rate and disk accretion rate at the disk formation time.

2. Protostellar collapse: Mass accretion rate

The mass accretion rate is explained in this section from the perspective of core mass and core accretion rate as described by Shu (1977). The core accretion rate was formulated in terms of isothermal sound speed, time and the mass contained in radius r. However, despite their importance in regulating the accretion rate of the core, some parameters were overlooked. Beginning with Shu (1977)'s basic equations, we intend to incorporate the effects of rotation, magnetic field and turbulence. Considering a cloud supported by thermal pressure with an isothermal sound speed of

$$a_t = \sqrt{\frac{k_B T}{\mu m_H}}, \tag{1}$$

where $k_B = 1.38 \times 10^{-23}\ \mathrm{m^2\,kg\,s^{-2}\,k^{-1}}$ is Boltzmann's constant, $\mu \approx 2.36$ is mean molecular weight of particle and m_H is mass of hydrogen atom. We intend to begin from the Shu (1977) model which is given by:

$$M(R,t) = \frac{a_T^3 t}{G} m(R), \tag{2}$$

where $t = 0$ is the instant when the mass of the core $M(0,t) = 0$ (the mass enclosed within radius R). An estimate of $\dot{M}_{\mathrm{acc}}$ requires the solution of dynamical collapse problem. In the idealized case of the collapse of a marginally unstable cloud, such a solution has been found semi-analytically by Shu (1977). In this theory, the accretion rate onto the protostar is:

$$\dot{M}_{\mathrm{acc}} = \alpha \frac{a_T^3}{G}, \tag{3}$$

this shows the gas free-falls onto a growing protostar at a constant rate, which depends only on the effective isothermal sound speed a_T and the gravitational constant G, where α is a constant with a magnitude of unity.

Inferring from (Shu 1977), the accretion rate of the turbulent core can be

$$\dot{M}_{\mathrm{acc}} \simeq \frac{(a_T^2 + v_A^2 + v_{\mathrm{turb}}^2)^{3/2}}{G},$$

where

$$v_{\rm turb} = \sqrt{\frac{p_{\rm turb}}{\rho}} \quad \text{and} \quad v_A = \frac{B}{\sqrt{4\pi\rho}}$$

are the turbulent and Alfvén speed, respectively. This (Shu 1977) model considers the non-rotating core. But in this work, we considered the rotating, magnetized and turbulent molecular cloud core. In dense cores with very little non-thermal support, the gas kinetic temperature varies between 10 and 30 K, corresponding to a_T = 0.1–0.3 km s^{-1},

$$t_{\rm acc} = \frac{M_\star}{\dot{M}_{\rm acc}} \gtrsim 10^5 \text{ yr}$$

(Shu 1977). We assumed the temperature of accreting core can vary beyond the values explained above. In this paper, we take into account parameters of the central star-forming core (protostar).

3. Protoplanetary disk formation and evolution

Protoplanetary disks are formed almost immediately after the collapse of a MC (Williams & Best 2014). As more material from the protostar with higher angular momentum begins to fall inward, the material will quickly flatten into a disk that surrounds the protostar. Let us consider a circular shell with radius r within a disk and calculate the rate of mass flow through the disk's inner edge with surface density Σ_d and $M_{in} = \pi r^2 \Sigma_d$ with $(dM_{in})/dt = 2\pi r \Sigma_d (dr/dt)$. Thus, we can write the mass accretion rate in the following form:

$$\dot{M}_{in} = 2\pi r \Sigma_d v_{(r)}, \tag{4}$$

where $\dot{M}_{in}$ is the mass in fall through the inner edge, $v(r)$ is the speed with which the infalling matter moves.

4. Theoretical model

4.1 *Magnetized, rotating and turbulent protostellar core accretion rate*

The total mass inside radius R (including core) at time t is $M(R, t)$ and it is the instantaneous mass, and $v(R, t)$ is the fluid velocity. We consider the motion of the fluid is influenced by the pressures due to thermal, magnetic, turbulence and rotation. These pressures contribute to this velocity. Therefore, we deduced the velocities of the fluid that originated from pressures as a_T, v_A, $v_{\rm turb}$ and a particle's velocity in the core as v, where $v^2 = \omega^2 R^2$. Consider that the accretion rate depends on temperature, magnetic field, turbulence and rotation of the disk. Due to this reason, we proposed the following relationship for the accretion rate of the disk and the protostar:

$$\dot{M}_{\rm acc} \simeq \left| \frac{(a_T^2 + v_A^2 + v_{\rm turb}^2 + \omega^2 R^2)^{3/2}}{G} \right|, \tag{5}$$

where R is the radius of the core. The RHS of Equation (7) indicates that the pressure inside the core reduces the matter falling on the central core. These pressures result in the speeds shown in Equation (7). This implies that thermal pressure is not the only pressure causing motion of particles or gases inside the core. The magnetic field, turbulence and rotation flatten the protoplanetary disk to conserve angular momentum. The pressure produced inside the core due to the magnetic field, turbulence and rotation of the core slows down the mass flow rate.

4.2 *Protostellar core mass and protoplanetary disk mass relation*

We assume that the core forms a single star surrounded by a disk and the core accretion rate can be approximated to the disk inner edge accretion rate. Then, we have:

$$\dot{M}_{in} = \dot{M}_{\rm acc} \tag{6}$$

implies

$$2\pi r \Sigma_d v_{(r)} = \frac{(a_T^2 + v_A^2 + v_{\rm turb}^2 + \omega^2 R^2)^{3/2}}{G}. \tag{7}$$

In this text, we use Σ_d, which is disk's surface density. Here, r is time dependent, however for simplicity, we use it as it is. The LHS of Equation (7) is property of the disk and the RHS of it is the property of the central core, therefore, according to this expression r and R are disk's and the core's radius, respectively, such that $(r > R)$. From Equation (7) we have:

$$(G 2\pi r \Sigma_d v_{(r)})^{2/3} = a_T^2 + v_A^2 + v_{\rm turb}^2 + \omega^2 R^2. \tag{8}$$

Here, we consider a spherical coordinate system with spherical magnetic field components given as $(B_r + B_\theta + B_\phi)$, where the magnitude of the magnetic field is $B = (B_r^2 + B_\theta^2 + B_\phi^2)^{1/2}$, so that we express the magnetic pressure inside the core using this magnetic field. Then, Equation (8) becomes

$$(G 2\pi r \Sigma_d v_{(r)})^{2/3} = \frac{K_{\rm B} T}{\mu m_H} + \frac{B^2}{4\pi\rho} + v_{\rm turb}^2 + \omega^2 R^2. \tag{9}$$

We can now multiply the RHS of Equation (9) by $(M_{\rm core})/(M_{\rm core})$ to get:

$$(G2\pi r\Sigma_d v_{(r)})^{2/3} = \frac{K_{\rm B}T}{\mu m_H}\frac{M_{\rm core}}{M_{\rm core}} + \frac{B^2}{4\pi\rho}\frac{M_{\rm core}}{M_{\rm core}} + v_{\rm turb}^2\frac{M_{\rm core}}{M_{\rm core}} + \omega^2R^2\frac{M_{\rm core}}{M_{\rm core}} \quad (10)$$

yields

$$(G2\pi r\Sigma_d v_{(r)})^{2/3} = \frac{1}{M_{\rm core}}\left(\frac{K_{\rm B}T}{\mu m_H}M_{\rm core} + \frac{B^2}{4\pi\rho}M_{\rm core} + v_{\rm turb}^2M_{\rm core} + \omega^2R^2M_{\rm core}\right). \quad (11)$$

This leads to

$$M_{\rm core}\left(G2\pi r\Sigma_d v_{(r)}\right)^{2/3} = \left(\frac{K_{\rm B}T}{\mu m_H}\frac{4\pi R^3}{3}\rho + \frac{B^2}{4\pi\rho}\frac{4\pi R^3}{3}\rho + v_{\rm turb}^2\frac{4\pi R^3}{3}\rho + \omega^2R^2\frac{4\pi R^3}{3}\rho\right), \quad (12)$$

$$VM_{\rm core}\left(G2\pi r\Sigma_d v_{(r)}\right)^{2/3} = \frac{4\pi R^3}{3} \times \left(\frac{K_{\rm B}T}{\mu m_H}\rho + \frac{B^2}{4\pi\rho}\rho + v_{\rm turb}^2\rho + \omega^2R^2\rho\right), \quad (13)$$

where $(4\pi R^3)/3$ and ρ are volume and density of the core, respectively, since $\rho = n\mu m_H$, thus we have:

$$M_{\rm core}\left(G2\pi r\Sigma_d v_{(r)}\right)^{2/3} = \frac{4\pi R^3}{3} \times \left(nK_{\rm B}T + \frac{B^2}{4\pi} + v_{\rm turb}^2\rho + \omega^2R^2\rho\right). \quad (14)$$

We rearrange $v_{\rm turb}^2\rho = P_{\rm turb}$, which is turbulence pressure in the core, then solve for $M_{\rm core}$, we get:

$$M_{\rm core} = \frac{\frac{4\pi R^3}{3}\left(nK_{\rm B}T + \frac{B^2}{4\pi} + P_{\rm turb} + \omega^2R^2\rho\right)}{\left(G2\pi r\Sigma_d v_{(r)}\right)^{2/3}}. \quad (15)$$

Equation (15) shows that the core mass is governed by the combination of dynamical parameters. We can also reformulate the mass of the core from Equation (15) using $t_{dcr} = r/v_{(r)}$ and $M_d = \pi r^2\Sigma_d$, then simplifying this, we arrive at:

$$M_{\rm core} = 1.230R^3\left(\frac{\pi t_{dcr}}{GM_d}\right)^{2/3} \times \left(nK_{\rm B}T + \frac{B^2}{4\pi} + P_{\rm turb} + \omega^2R^2\rho\right), \quad (16)$$

where n is the particle number density of the core, T is the core's temperature, and B is the core's magnetic field, ω is the angular velocity of the core, R is the core's radius, $\omega^2R^2 = v_\phi$ is the rotational velocity of the core, ρ is the density of the core, and M_d is the disk's mass. Then, the disk mass can be given by:

$$M_d = (1.230R^3)^{3/2}\frac{\pi t_{dcr}}{G}M_{\rm core}^{-3/2} \times \left(nK_{\rm B}T + \frac{B^2}{4\pi} + P_{\rm turb} + \omega^2R^2\rho\right)^{3/2}. \quad (17)$$

Using $J_{\rm core} = M_{\rm core}\omega_{\rm core}R^2$ we have:

$$M_d = (1.230R^3)^{3/2}\frac{\pi t_{dcr}}{G}M_{\rm core}^{-3/2} \times \left(nK_{\rm B}T + \frac{B^2}{4\pi} + P_{\rm turb} + \frac{\omega_{\rm core}J_{\rm core}}{M_{\rm core}}\rho\right)^{3/2}. \quad (18)$$

This yields

$$M_d = (1.230R^3)^{3/2}\frac{\pi t_{dcr}}{G}M_{\rm core}^{-3/2} \times \left(nK_{\rm B}T + \frac{B^2}{4\pi} + P_{\rm turb} + \frac{3\omega_{\rm core}J_{\rm core}}{4\pi R^3}\right)^{3/2}, \quad (19)$$

where $P_{\rm turb}$ and $B^2/8\pi = P_m$ are the turbulent and magnetic pressure inside the core. Equation (19) shows that $M_d \propto M_{\rm core}^{-3/2}$. This indicates that the disk mass reduces as the core mass grows because the mass is engulfed by the core from the surrounding disk. However, when the pressures inside the core become stronger, the rate of mass infall reduces and there can be an outflow of gases due to the core radiation. The fastest rotating central core leads to the fastest disk mass growth. From Equation (19) we get:

$$M_d = \frac{1.3641\pi t_{dcr}R^{9/2}}{G}M_{\rm core}^{-3/2}\left(nK_{\rm B}T + \frac{B^2}{4\pi} + \rho v_{\rm turb}^2 + \frac{0.2387\omega_{\rm core}^2M_{\rm core}}{R}\right)^{3/2}. \quad (20)$$

Equation (20) shows the relation between disk mass and core mass is power-law with an index of $-3/2$. We see from this equation the net effect of these pressures reduce the accretion of matter onto the central core. This leads to the growth of mass of protoplanetary disk that surrounds the central protostar.

4.3 *Angular momentum transfer*

The falling of matter onto the central core continues until the young star's temperature gets high enough to begin nuclear fusion. The accretion of material onto the newly formed star must be accompanied by an expansion of the remaining disk material to conserve angular

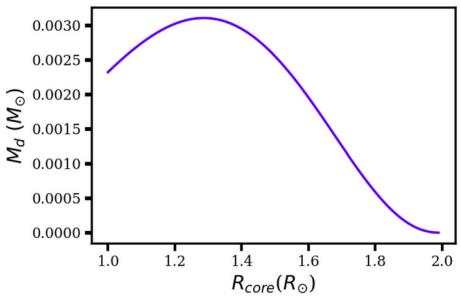

Figure 1. Core radius vs. disk mass was plotted using Equation (20) for $M_{\rm core} = 1$–$1.09\ M_\odot$.

momentum. Thus:

$$J_{\rm core} = J_d, \tag{21}$$

where $J_{\rm core}$ and J_d are the angular momenta of the core and the disk

$$M_{\rm core}\omega_{\rm core}R^2 = M_d\omega_d r^2. \tag{22}$$

Using Equations (22), we get:

$$J_d = \frac{1.3641\pi t_{dcr}\omega_d R^{9/2}r^2}{G}M_{\rm core}^{-3/2}\left(nK_{\rm B}T + \frac{B^2}{4\pi} + \rho v_{\rm turb}^2 + \frac{0.2387\omega_{\rm core}^2 M_{\rm core}}{R}\right)^{3/2}. \tag{23}$$

From Equation (23), we see that the contributions from all the four parameters, thermal and non-thermal (turbulent) pressures, magnetic field pressure and core rotation inside the core increase the disk angular momentum.

4.4 *Analytic results*

The parameter intervals given below were used to plot our analytical results. The parameters are chosen along with their values from the predetermined ranges by Enoch *et al.* (2009), Walch *et al.* (2010), Armitage (2010), Ward & Whitworth (2011), Mann *et al.* (2015); for example, if a core of $R = 1.99$–$1\ R_\odot$, with $\rho = 10^{-3}$–10^{-1} kg m^{-3} and the disk crossing time is $Vt = 10^3$–10^5 yr, $T = 1000$–$10{,}999$ K, $\omega_{\rm core} = 10^{-14}$–$10^{-12}$ s^{-1}, $\omega_d = 10^{-15}$–10^{-13} s^{-1}, $B = 10^{-3}$–10^{-2} G, $n = \rho_{\rm core}/\mu m_H$, $v_{\rm turb} = 400$–499 ms^{-1}, $M_{\rm core} = 0.1$–$1.09\ M_\odot$ and $r = 10$–109 au. Figures are plotted using these intervals.

Figures 1 and 2 indicate the relationship between the core properties and a protoplanetary disk that surrounds the central core. We understand from Figure 1 that at the early disk formation time, the disk mass increases as the core radius grows, but after a moment, if the core radius increases, the disk mass falls because the core may engulf the matter from the disk. As the time goes, the mass provided from the surrounding cloud to the disk may reduce. As Figure 2 indicates that the disk mass grows with the core mass until the core mass reaches >60% of its own final mass, at which point the disk mass begins to fall as the core mass is greater than this percentage of the final mass. Both figures imply that the dynamic processes going on inside the core influence the protoplanetary disk's mass and the final planetary disk as well. This may result in a smaller protoplanetary disk mass as the central star-forming core grows larger.

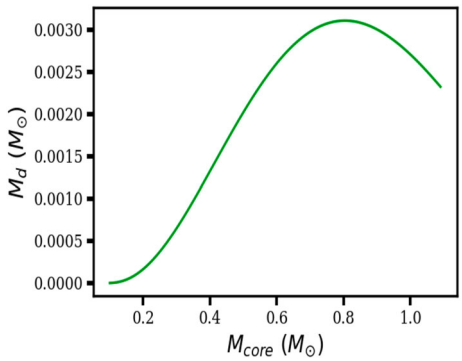

Figure 2. Core mass vs. the surrounding protoplanetary disk mass plotted using Equation (20) for $M_{\rm core}$=1–$1.09\ M_\odot$.

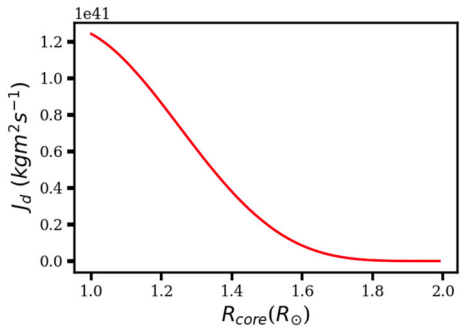

Figure 3. Core radius vs. disk angular momentum using Equation (23) for $M_{\rm core} = 1$–$1.09\ M_\odot$.

Figures 3 and 4 show the central core radius and mass vs. the protoplanetary disk angular momentum, respectively. Figure 3 shows the momentum of the disk reduces as the core radius increases up to some values and then begins to stay constant after the formation of the planetary disk. Moreover, as the core mass increases, the disk angular momentum develops (see Figure 4).

5. Observational results for comparison

In this section, we intended to test our theory by deriving the masses of the observed disks. We compiled the available data from the literature and used the

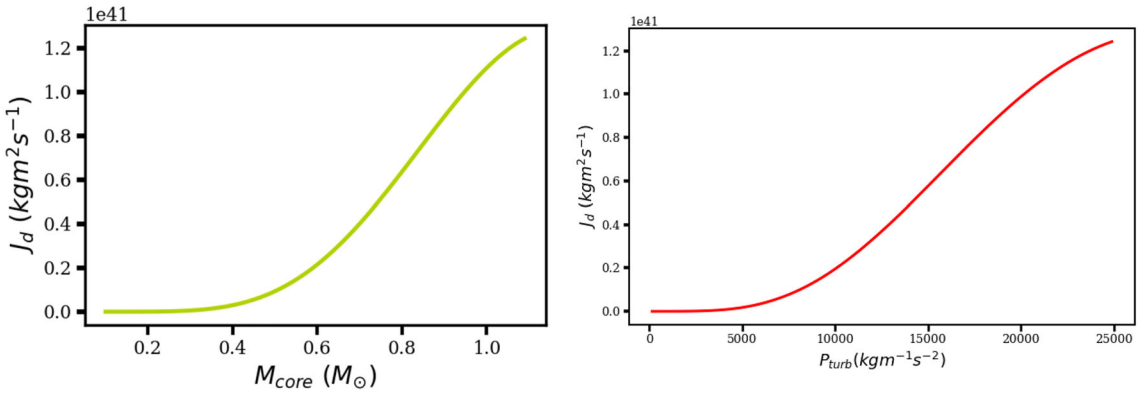

Figure 4. Core mass vs. disk angular momentum (left panel) and core's turbulence pressure vs. the disk's angular momentum (right panel) considering r_d = 1–109 au.

observed disk fluxes and dust luminosities from Kenyon & Bromley (2010) to calculate the protoplanetary disks' mass surrounding stars of 1–3 $M_\odot$. To determine the disk mass surrounding a young, newly formed star, we, therefore, assume a uniformly bright, spherical disk flux, which is given by:

$$F_\nu = \pi B_\nu \left(\frac{R}{d}\right)^2. \tag{24}$$

By assuming optically thin emission and an isothermal disk with a dust temperature of T_d = 20 K, Cox *et al.* (2017) modeled disk mass as:

$$M_d = \frac{F_\nu d^2}{\kappa_\nu B_\nu(T_d)}, \tag{25}$$

where F_ν is the integrated flux at 870 μm, d is the estimated distance to Ophiuchus (Cox *et al.* 2017) and κ_ν = 0.03 cm^2 g^{-1} is the total opacity at 870 μm assumed as of Cox *et al.* (2017) and B_ν is the Planck function. An estimation of 100:1 gas-to-dust ratio (Cox *et al.* 2017) has been used. However, recent studies have suggested that the gas mass might be considerably lower than the often prescribed 100:1 ratio (Williams & Best 2014). In this paper, we adopt the disk mass modeled by Cox *et al.* (2017) to drive our own equation of the disk mass using relative fluxes at a given micron and dust luminosities.

5.1 *Disk mass from its flux and luminosity*

The reason why we need to derive the equation of the disk mass in terms of flux and luminosity is the accessibility of the data on the flux and luminosity of disks. To calculate the protoplanetary disk mass surrounding low to intermediate-mass stars from their observational values of flux and luminosity, we have to formulate disk mass in terms of flux and luminosity, beginning from the known equations of disk mass. So, in the first place, inserting Equation (26) into Equation (27) and using the Rayleigh–Jeans approximation of the mass of the protoplanetary disk in terms of its radius and opacity is:

$$M_d = \frac{\pi R_d^2}{\kappa_\nu}. \tag{26}$$

For simplicity,

$$\pi R_d^2 = \frac{L_d}{4F_d}, \tag{27}$$

where R_d, L_d and F_d are the disk radius, disk luminosity and disk flux, respectively. From Equation (29), we get:

$$R_d = \sqrt{\frac{L_d}{4\pi F_d^{i\ (\mu m)}}}. \tag{28}$$

In our case, $F_d^{i\ (\mu m)}$ represents the relative disk flux at i microns, where i can be 850 μm or other value, but it is based on the data we have been using. Again, combining Equation (26) into Equations (27) and (28), the disk mass from luminosity and flux is described by:

$$M_d = \frac{L_d}{4F_d^{i\ (\text{microns})}\kappa_\nu}. \tag{29}$$

The subscript d is read as a disk, whereas F^i is the flux of the disk at a given i micron. From Equation (29), we see that the disk mass depends on the dust luminosity and the relative disk flux at a given micron. Therefore, to obtain the mass of the disk surrounding a given star observed at a particular IR waveband (IR wavelength range), one can apply this model (Equation 29). So, we applied this method to determine the mass of the protoplanetary disk rounding a given observed star using the data publicly available.

Table 1. Calculated at the relative maximum dust luminosities and the relative maximum disk fluxes at 850 microns for disks rounding 1–3 $M_\odot$ using model (Equation 29) and data of Kenyon & Bromley (2010).

Host star ($M_\odot$)	$\log F^{850\ (\mu m)}$ (J s^{-1} cm^{-2})	$\log(L_d)$ ($L_\odot$)	M_d ($M_\odot$)
1	2.059	2.256	7.80×10^{-4}
1.5	1.878	2.260	0.0013
2	1.714	2.180	6.56×10^{-4}
2.5	1.804	2.326	0.0014
3	0.820	1.400	0.0012

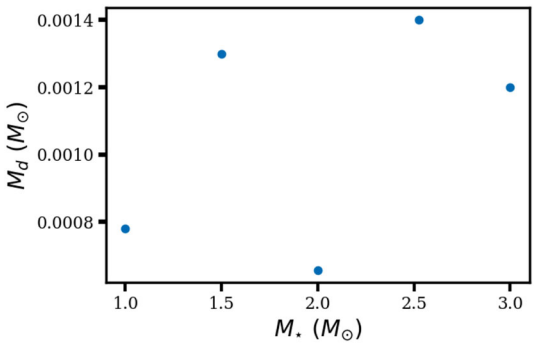

Figure 5. Relative disk masses of the host star with masses 1–3 $M_\odot$ stars at 850 microns are calculated using Equation (29) from the relative maximum fluxes and maximum luminosities (Table 2).

5.2 *Relation between protoplanetary disks and their host star from data*

Applying Equation (29), we calculated the mass of the protoplanetary disk surrounding protostars of masses 1–3 $M_\odot$ at the maximum fluxes and maximum luminosities as well as at the minimum fluxes and minimum luminosities from the data of disks (Kenyon & Bromley 2010). Accordingly, we calculated disks' masses for the relative maximum values of fluxes and luminosities and for the relative minimum values as well. We adopted the opacity value suggested by Cox *et al.* (2017), which is $\kappa_\nu \approx 0.03$ cm^2 g^{-1} for flux at 870 microns and approximate it with κ_ν of 850 microns. The relative dust luminosity is maximum approximately at the disk age of 10^7–$10^{7.5}$ yr for both disks surrounding 1–3 $M_\odot$ stars according to the values obtained from the data. For the star mass (3 $M_\odot$), its disk luminosity seems constant after its peak value for some time (Table 1).

As we see the results in Figure 6 and Table 2, the disk mass is not directly dependent on the stellar mass. For the relative maximum flux and luminosity, the massive disk obtained is 2.5 $M_\odot$ and the second massive disk is 1.5 $M_\odot$ relatively. The differences may be raised due to their radii, which influence their luminosities. This shows that the disk properties depend on the properties of the core (parent cloud) as indicated in our theoretical model. Therefore, we formulated the theoretical models to indicate the relationship between the disk and its hosting star's properties are in agreement with the results and analysis suggested by Kenyon & Bromley (2010) from the data. Figure 5 shows no direct relation between the protoplanetary disk and its hosting star mass in this particular situation. This implies that observing relative maximum values of disk flux and dust luminosity do not necessarily mean that the disk mass rounding more massive star is massive.

Table 2. Calculated disk mass at the relative minimum dust luminosities and the relative minimum disk fluxes at 850 microns for disks rounding 1–3 $M_\odot$. Using data, which was made public by Kenyon (2008), the disk's mass is calculated using Equation (29).

Host star ($M_\odot$)	$\log(F)$ (J s^{-1} cm^{-2})	$\log(L_d)$ ($L_\odot$)	M_d ($M_\odot$)
1	0.070	4.980	1.4483×10^{-4}
1.5	0.072	4.930	1.6175×10^{-4}
2	0.072	4.740	2.5053×10^{-4}
2.5	0.054	4.660	3.1394×10^{-4}
3	0.046	4.670	3.125×10^{-4}

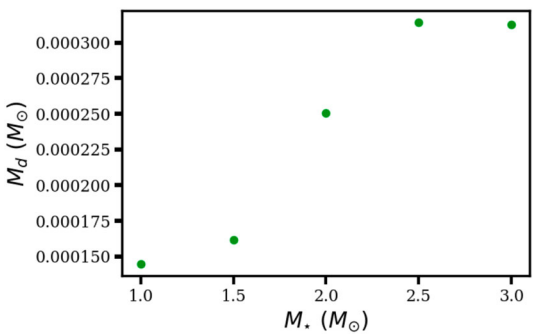

Figure 6. Relative masses of the disks of host star mass range from 1 to 3 $M_\odot$ stars at 850 microns for the relative minimum fluxes and minimum luminosities.

The disk mass calculated using the relative minimum flux and minimum luminosity of disks rounding 1–3 $M_\odot$ is increasing with stellar mass (Figures 6 and 7). Now link the theoretical result that we obtained using Equation (26) with the method of calculating disk mass from flux and luminosity and taking the average value of the minimum and maximum disk mass rounding star of

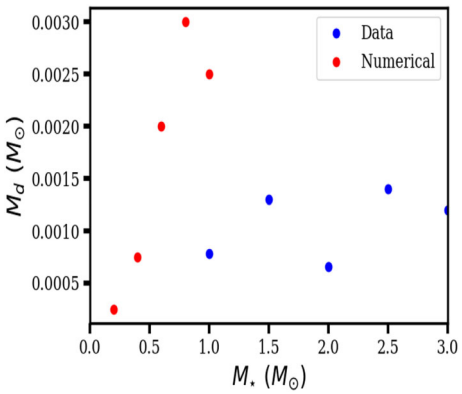

Figure 7. Blue dots represent the observed relative disk mass at 850 microns rounding 1–3 $M_\odot$ stars calculated using Equation (29) from the relative maximum fluxes and maximum luminosities. The red dots are numerical results calculated using our theoretical model. This graph shows that the maximum disk mass is obtained for 0.8 $M_\odot$ in the model, while the observational data shows the disk with larger mass is surrounding star of 2.5 $M_\odot$.

2 $M_\odot$, we found the disk mass rounding this type of star using our theoretical result is $M_d \approx 4.5323 \times 10^{-4}\ M_\odot$. So, our model can help us to predict the mass of the star and disk that will form from the currently evolving disk, core and protostellar core.

From Figure 6, we see that the disk mass is increasing with stellar mass. The graph is plotted from Table 2, which is obtained from Equation (29) and data from Kenyon (2008). This figure shows the disk mass calculated from relative minimum disk flux and dust luminosity is almost dependent on its hosting star's mass. Therefore, observing minimum disk flux and dust luminosity rounding relatively massive star will result in a massive disk.

If the central protostar is strongly magnetized, the magnetic field can create strong magnetic pressure, which reduces the infalling rate of matter then the surrounding disk may get enough materials to develop as a protoplanetary disk. Moreover, strong turbulence can protect the falling of gases and dust onto the central protostar. This also leads to enhancing the flattening of the protoplanetary disk to conserve angular momentum.

6. Comparison of theoretical and observational results

We calculated the theoretical results of disk mass and its hosting star using our models, such as Equations (16) and (20) through fixing as well as varying the parameters in those equations. Then, we plotted the numerical and the observational results calculated from the relative maximum flux and maximum luminosity as well as the relative minimum flux and minimum luminosity as shown in Figures 6 and 7.

7. Conclusions

We investigated the protoplanetary disk formation in magnetized, turbulent and rotating cloud cores. To formulate and calculate the disk mass, we use the core and the disk accretion rate to obtain the relation between the disk and properties of the central protostar. The rotation, magnetic field and turbulence of the central protostar is triggering the growth of the surrounding disk mass and angular momentum of the protoplanetary disk. However, if magnetic field of the protoplanetary disk is getting stronger, it will hinder the disk mass growth through stopping (reducing) the infalling of matter from the envelop to the protoplanetary disk.

We have calculated the disk mass at the relative maximum dust luminosities and the relative maximum disk fluxes at 850 microns for disks surrounding protstar of 1–3 $M_\odot$ almost leads to a larger disk mass relative to those of the minimum values of the flux and luminosities. This suggests that the massive disk has a higher dust luminosity and disk flux.

We plotted the relative disk mass rounding 1–3 $M_\odot$ stars at 850 microns in Figure 5 using the relative maximum fluxes and maximum luminosities from Equation (29). The figure shows no direct relation between the protoplanetary disk mass and its hosting star mass in this particular situation. This implies that observing relative maximum values of disk flux and dust luminosity do not necessarily mean that the disk mass rounding more massive star is massive.

We show in Figure 6 that the disk mass calculated from relative minimum disk flux and dust luminosity is almost dependent on its hosting star's mass. Therefore, observing minimum disk flux and dust luminosity rounding relatively massive star will result in a massive disk.

Figure 7 shows that the maximum disk mass is obtained for $\sim$0.8 $M_\odot$ in the model, while the observational data shows the more massive disk is found surrounding star of 2.5 $M_\odot$. This difference happens due to rotation, magnetic field and turbulence that have been considered in the model. Therefore, the environment in which disk forming cloud dwelling in, can affect the mass of the disk that formed surrounding a given star. The results tell us that the dynamical processes involving disk and the host star formation can play great role

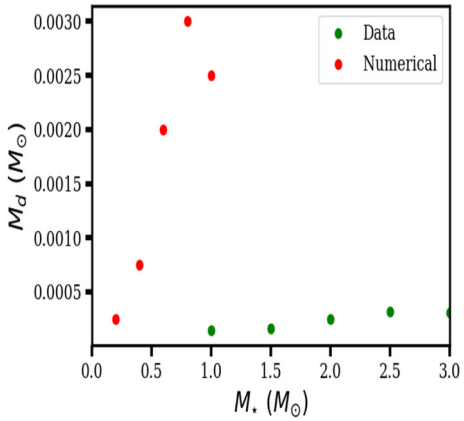

Figure 8. Green dots represent the observed relative disk mass at 850 microns rounding 1–3 $M_\odot$ stars calculated using Equation (29) from the relative minimum fluxes and minimum luminosities. The red dots are numerical results that are generated numerically from our theoretical model. This graph shows that the result is appropriate for the stellar mass of 1–2 $M_\odot$.

in the disk mass growth. Moreover, the results confirm that there is an interplay among many dynamic processes and parameters in determining disk and host star relations.

However, in Figure 8, the disk mass obtained from the relative minimum disk flux and minimum dust luminosity is larger in mass than that of our theoretical result as compared to that of the maximum flux and luminosity. As a result, the numerical calculation performed in this paper agrees more with the observational result obtained from maximum disk flux and maximum dust luminosity. So, the core properties can influence the final mass of the protoplanetary disk formed.

Acknowledgements

We gratefully acknowledge Space Science and Geospatial Institute (SSGI), Entoto Observatory and Research Center (EORC), Department of Astronomy and Astrophysics. East African Astrophysics Research Network (EAARN) and International Science Programme (ISP)-Uppsala University are also gratefully recognized for their support this research.

References

Ansdell M., Williams J. P., van der Marel N. *et al.* 2016, PVizieR Online Data Catalog, J/ApJ/828/46
Anathpindika S., Di Francesco J. 2013, MNRAS, 430, 1854
Armitage P. 2010, AAS, 216, 108
Bate M. 1998, Brown Dwarfs and Extrasolar Planets, 134, 273
Cassen P., *et al.* 2006, Extrasolar Planets: Swiss Society for Astrophysics and Astronomy 369
Cox E. G., Harris R. J., Looney L. W. *et al*. 2017, ApJ, 851, 83
Enoch M. L., Corder S., Dunham M. M. *et al*. 2009, ApJ, 707, 103
Gonzalez J.-F., Laibe G., Maddison S. T., Pinte C., Menard F. 2015, Monthly Notices of the Royal Astronomical Society: Letters, 454, L36
Inutsuka S.-I., Machida M. N., Matsumoto T. 2010, ApJ, 718, L58
Joos M., Hennebelle P., Ciardi A. 2012, A&A, 543, A128
Kenyon S., Bromley B. 2010, VizieR Online Data Catalog, J/ApJS/188/242
Kimura S. S., Tsuribe T. 2012, PASJ, 64, 116.
Mann R. K., Andrews S. M., Eisner J. A. *et al*. 2015, ApJ, 802, 77
Matsumoto T., Hanawa T. 2003, ApJ, 595, 913
Najita J. R., Andrews S. M., Muzerolle J. 2015, MNRAS, 450, 3559
Nakamoto T., Nakagawa Y. 1994, ApJ, 421, 640.
Nixon C. J., Hands T. O., King A. R., Pringle J. E. 2018, MNRAS, 477, 3539
Nomura H., Tsukagoshi T., Kawade R. *et al*. 2016, ApJ, 819, L7
Oppenheimer J. R., Volkoff G. M. 1934, Physical Review, 55, 374.
Seifried D., Banerjee R., Pudritz R. E., Klessen R. S. 2013, MNRAS, 432, 3320
Shu F. H. 1977, ApJ, 214, 488
Walch S., Naab T., Whitworth A., Burkert A., Gritschneder M. 2010, MNRAS, 402, 2253
Ward-Thompson D., Whitworth A. P. 2011, An Introduction to Star Formation (Cambridge University Press)
Williams J. P., Mann R. K., Di Francesco J. *et al.* 2014, ApJ, 796, 120
Zhang Q., Qiu K., Girart J. M. *et al*. 2014, ApJ, 792, 116
Zhu Z., Hartmann L., Gammie C. F. *et al*. 2010, ApJ, 713, 1134